

User-Centric Perspective in Random Access Cell-Free Aided by Spatial Separability

Victor Croisfelt, Taufik Abrão, José Carlos Marinello Filho

Abstract—In a cell-free massive multiple-input multiple-output (mMIMO) network, multiple access points (APs) actively cooperate to serve users' equipment (UEs). We consider how the problem of random access (RA) to pilots can be addressed by such a network under the occurrence of pilot collisions. To find a solution, we embrace the user-centric perspective, which basically dictates that only a preferred subset of APs needs to service a UE. Due to the success of the strongest-user collision resolution (SUCRe) protocol for cellular mMIMO, we propose an extension of SUCRe considering the new setting. During the extension process, we observe that the user-centric perspective naturally equips a cell-free network with a method for resolving collisions. We refer to this method as spatial separability, which comes from the macro-diversity brought about by the additional AP dimension. We then propose two novel RA protocols for cell-free mMIMO: i) the baseline cell-free (BCF) that resolves collisions with the concept of separability alone and ii) the cell-free SUCRe (CF-SUCRe) that combines SUCRe and spatial separability to resolve collisions. We evaluate our proposed RA protocols against the cellular SUCRe (Ce-SUCRe). The BCF and CF-SUCRe perform $6\times$ to $2\times$ better on average compared to the Ce-SUCRe with an average energy efficiency gain of $45\times$ to $125\times$, respectively. Among our methods, even with a higher overhead, the CF-SUCRe is superior to BCF because the combination of methods for collision resolution allows many APs to be disconnected from RA without sacrificing much performance.

Index Terms—Cell-Free; User-Centric; Random Access; Spatial Separability; 6G systems

I. INTRODUCTION

IN future mobile networks, massive wireless connectivity is a fundamental requirement sought to support the expected huge amount of users' equipment (UEs) [1], [2]. As a consequence, the task of improving the performance of random access (RA) to the network has been the focus of considerable research [2]. Recently, cellular massive multiple-input multiple-output (mMIMO) technology has proven to be a great ally in achieving these improvements with, for example, the introduction of the strongest-user collision resolution (SUCRe) protocol in [3]. SUCRe exploits the channel hardening and favorable propagation capabilities of cellular mMIMO systems. Exploring these features allows for a distributed resolution of collisions that occur due to pilot shortage. The success of the SUCRe protocol resulted in the proposition of several variants that seek to solve problems of the original SUCRe [3] (see [4] and references therein), such as the unfairness caused by the

fact that UEs closer to the base station (BS) are more likely to be favored by the protocol.

As the requirements of future mobile networks become increasingly challenge, new technologies has been gaining attention in addition to cellular mMIMO. In [5], the authors introduce the concept of extra-large-scale MIMO or XL-MIMO by arguing that cellular mMIMO operates differently when the size of the antenna arrays is very large. Remarkably, the authors of [6] adapted the SUCRe protocol for XL-MIMO systems. Another promising approach is to completely get rid of the cellular perspective of design, giving rise to the notion of cell-free mMIMO networks [7]. In these systems, a UE is surrounded by now called access points (APs) that actively cooperate with each other and also make use of the principles behind mMIMO technology. In particular, we are interested in the *user-centric perspective* of cell-free networks [7], where a UE is served by a preferred subset of APs that are presumably closer to it, allowing for better computational scalability of the network. Since cell-free mMIMO has been gaining greater interest only recently, there are few works that discuss the problem of RA under this scenario [8]–[11].

In this work, we propose an extension of the SUCRe protocol for cell-free mMIMO networks. Our motivation comes from the lack of protocols in the literature that adequately explore the cell-free architecture and the user-centric perspective. Furthermore, we emphasize the interest in grant-based RA protocols, which are justified when the size of the information to be transmitted by UEs is large enough, like in crowded enhanced mobile broadband services [3]. Alternatively, grant-free protocols are intended for application scenarios in which the communication of UEs is very sporadic and short, such as in massive machine-type communications [2].

A. Relevant Prior Work

There are few works that discuss the RA problem in cell-free mMIMO networks [8]–[11]. In [8] and [11], the authors proposed a grant-free protocol based on activity detection using the maximum likelihood method, showing the first traces of RA performance gains with cell-free architecture. These improvements are intrinsically obtained by exploiting the *macro-diversity* introduced by the existence of diverse geographically distributed APs. Of course, the price to pay for macro diversity is the implementation of further infrastructure to support the cell-free architecture. Following the same line of work from [8], the papers [9] and [10] use other mathematical frameworks to introduce more efficient algorithms to obtain a grant-free protocol considering activity detection. Contrastingly, our work considers the design of a grant-based protocol for cell-free mMIMO primarily based on the SUCRe principle for collision resolution.

V. Croisfelt is with the Electrical Engineering Department, Universidade de São Paulo, Escola Politécnica, São Paulo, Brazil; victorcroisfelt@usp.br

T. Abrão is with the Electrical Engineering Department, State University of Londrina, PR, Brazil. E-mail: taufik@uel.br

J. C. Marinello is with the Electrical Engineering Department, Universidade Tecnológica Federal do Paraná, Cornélio Procópio, PR, Brazil. E-mail: jcmarinello@utfpr.edu.br

B. Our Contributions

In this paper, we extend the SUCRe protocol [3] for cell-free mMIMO networks. This extension aims to fully exploit the user-centric perspective [7], that is, *not all APs necessarily need to service all RA pilots and not even be operational on the RA as a whole*. Because of this, the proposed extension is not immediate, requiring the introduction of several new concepts. The salient features of our extension are:

- 1) We introduce the notions that: **a)** a UE is only aware of a preferred subset of APs and **b)** another preferred subset of APs is allocated by the cell-free network to serve each RA pilot. Through the introduction of these, we change the steps of the original SUCRe [3] in such a way as to preserve the desired property that collisions are resolved in a *decentralized* way by each of the UEs.
- 2) The difference between the preferred subsets of APs of each UE and the preferred subset of APs servicing each pilot generates a particular macro-diversity for the cell-free architecture. We observe that one can exploit this macro-diversity to solve pilot collisions. We refer to this way of resolving pilot collisions as *spatial separability*.
- 3) To allow the application of the SUCRe in a decentralized way, we propose and exhaustively evaluate three estimators. The design of these estimators needs to take into account that a UE only knows its preferred subset of APs, which is different from the subset of APs that service the RA pilot sent by it.
- 4) Altogether, we present two RA protocols in this work: **i)** a grant-free protocol named as *baseline cell-free* (BCF) which only exploits the spatial separability concept to resolve collisions and **ii)** a grant-based protocol called *cell-free SUCRe* (CF-SUCRe) which combines SUCRe and spatial separability concepts to resolve collisions.

Our main result is that, despite being a grant-based protocol, CF-SUCRe performs as well as the BCF, although it is more energy efficient. The reason for this is that the combination of SUCRe and spatial separability allows to reduce the amount of APs that need to be operating in the RA without affecting the performance of the RA as much. Henceforth, we refer to the original SUCRe by [3] as the *cellular SUCRe* (Ce-SUCRe).

C. Notation

Let \mathbb{R}_+ be the set of positive real numbers and \mathbb{C} be the set of complex numbers. Integer sets are denoted by calligraphic letters \mathcal{A} with cardinality given by $|\mathcal{A}|$ and empty set \emptyset . Lower case boldface letters denote column vectors (e.g., \mathbf{x}), while uppercase boldface letters stand for matrices (e.g., \mathbf{A}). The identity matrix of size N is \mathbf{I}_N , whereas $\mathbf{0}$ and $\mathbf{1}$ stands for a vector of zeros and ones, respectively. The Euclidean norm of an arbitrary vector \mathbf{x} is $\|\mathbf{x}\|_2$, while $\|\mathbf{x}\|_1$ is its l_1 -norm. The $\text{argsort}(\cdot)$ function sorts and returns the indices of a vector in ascending order. The ceil function is $\lceil \cdot \rceil$. The circularly-symmetric complex Gaussian distribution is denoted as $\mathcal{N}_{\mathbb{C}}(\cdot)$. Operators for probability and expectation are $\mathbb{P}\{\cdot\}$ and $\mathbb{E}\{\cdot\}$, respectively. In algorithm pseudo-codes, $==$ and $!=$ are used for equal and not equal comparisons, respectively. Further, \leftarrow

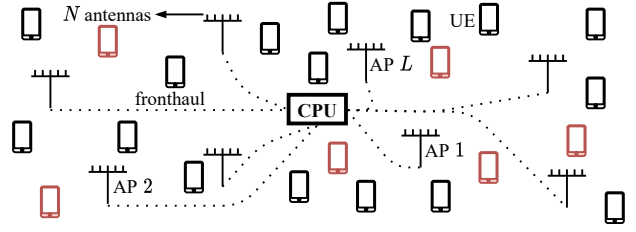


Fig. 1. Illustration of the system model. Red UEs represent the portion $\mathcal{K} \subset \mathcal{U}$ of inactive UEs that want to connect to the network, while black UEs remain idle. Fronthaul links are assumed to have unlimited capacity and provide error-free communication.

denotes assignment to a variable and $\text{sum}(\cdot)$ defines a function that sums Boolean values, where "True" is 1 and "False" is 0.

II. SYSTEM MODEL

Suppose that a subset $\mathcal{K} \subset \mathcal{U}$ of inactive UEs requests access to a cell-free mMIMO network comprised of L APs at a given moment. The APs are equipped with N antennas each and are indexed by $\mathcal{L} = \{1, 2, \dots, L\}$. A central processing unit (CPU) coordinates the exchange of information between APs through fronthaul links. Fig. 1 illustrates the adopted system model. We let P_a be the *probability of access* that dictates whether an inactive UE $k \in \mathcal{U}$ tries to access the network or not, i.e., whether k is a member of \mathcal{K} . We assume that the RA occurs through the transmission of pilots. The pilot pool $\Phi \in \mathbb{C}^{\tau_p \times \tau_p} = [\phi_1, \phi_2, \dots, \phi_{\tau_p}]$ contains τ_p pilots indexed by $\mathcal{T} = \{1, 2, \dots, \tau_p\}$. The pilots have the following properties: a) *normalized pilots* $\|\phi_t\|_2^2 = \tau_p, \forall t \in \mathcal{T}$ and b) *orthogonal pilots* $\phi_t^H \phi_{t'} = 0, \forall t \neq t',$ such that $t, t' \in \mathcal{T}$. The pilot pool is shared by all L APs and $|\mathcal{U}|$ inactive UEs with $\tau_p \ll |\mathcal{U}|$. Because of this sharing, *pilot collisions* happen whenever two or more UEs in \mathcal{K} choose simultaneously the same pilot t to request access to the network.

A. Channel Model

Let $\mathbf{h}_{kl} \in \mathbb{C}^N$ denote the channel vector between UE $k \in \mathcal{K}$ and AP $l \in \mathcal{L}$. For simplicity, we assume uncorrelated Rayleigh fading channels,

$$\mathbf{h}_{kl} \sim \mathcal{N}_{\mathbb{C}}(\mathbf{0}, \beta_{kl} \mathbf{I}_N), \forall (k, l), k \in \mathcal{K}, l \in \mathcal{L}.$$

The *average channel gain* β_{kl} is modeled according to

$$\beta_{kl} \in \mathbb{R}_+ = \Omega \cdot d_{kl}^{-\zeta}, \quad (1)$$

where Ω is a positive multiplicative power constant, d_{kl} is the distance in meters between UE k and AP l , and ζ is the pathloss exponent.

III. CF-SUCRE PROTOCOL

According to [3], the Ce-SUCRe protocol is comprised of four main steps and one preliminary step known as Step 0. Below, we adapt these steps to a cell-free mMIMO network, giving rise to the CF-SUCRe protocol. Our goal is to eagerly explore the user-centric perspective when performing such extension [7].

A. Step 0: Estimating Average Channel Gains

In this preliminary step, the k -th UE estimates its average channel gains $\beta_{k1}, \beta_{k2}, \dots, \beta_{kL}$ relying on control beacons sent by the L APs for $k \in \mathcal{U}$. For this estimation to be possible, we assume that the control signaling of the APs are orthogonal to each other. We also assume that a UE $k \in \mathcal{U}$ is only capable of perfectly estimating a β_{kl} if and only if $q_l \beta_{kl} > \iota \cdot \sigma^2$ for $l \in \mathcal{L}$, where q_l is the downlink (DL) transmit power of AP l , $\iota \in \mathbb{R}_+$ is a multiplicative constant such that $\iota \geq 1$, and σ^2 is the noise power. For simplicity, we suppose that q_l is the same for every AP $l \in \mathcal{L}$. Then, the k -th UE is aware of the average channel gains β_{kl} 's from the subset of APs denoted as $C_k \subset \mathcal{L}$ and defined by $C_k = \{l : q_l \beta_{kl} > \iota \cdot \sigma^2, \forall l \in \mathcal{L}\}, \forall k \in \mathcal{U}$.

The physical interpretation of the subset C_k is that it represents the APs closer to the k -th UE. To see this, by using (1), we can write the inequality $q_l \beta_{kl} > \iota \cdot \sigma^2$ as a function of the distance d_{kl} , yielding in

$$d_{kl} < \left(\frac{1}{\iota} \cdot \frac{\Omega \cdot q_l}{\sigma^2} \right)^{\frac{1}{\zeta}}. \quad (2)$$

This means that C_k can be geometrically interpreted as the subset of APs whose APs have distances relative to the k -th UE less than the *limit distance* or *limit radius* given by

$$d_k^{\text{lim}} = d_k^{\text{lim}} = \left(\frac{1}{\iota} \cdot \frac{\Omega \cdot q_l}{\sigma^2} \right)^{\frac{1}{\zeta}}. \quad (3)$$

Note that we can drop the subscript k of the limit radius. Further, the limit radius is as large as possible when $\iota = 1$. Consequently, the larger the ι , the smaller is d_k^{lim} and the fewer are the elements that comprise C_k . Particularly, the circular region around a UE with radius d_k^{lim} can be interpreted as the region which contains the APs that most influence a UE's communication, namely, the *UE's influence region*.

In the worst case, we assume that $|C_k| \geq 1$ APs irrespective of the value of ι , meaning that at least one AP has to be known so that a UE $k \in \mathcal{U}$ can try to access the network given a probability of access P_a . Henceforth, we denote as \check{C}_k the so-called *natural* subset C_k of known APs by UE k obtained when $\iota = 1$. The natural subset \check{C}_k corresponds to the APs within the circular area delimited by the largest radius in (3), representing the influence region of a UE in its fullness.

B. Step 1: Pilot Transmission and Pilot Activity

At a given instant, each one of the $|\mathcal{K}|$ UEs selects a pilot symbol $\phi_t \in \mathbb{C}^{\tau_p}$ at random from the pilot pool Φ . For UE $k \in \mathcal{K}$, this random selection is denoted as $c(k) \in \mathcal{T}$. The $|\mathcal{K}|$ UEs then transmit their chosen pilots in a broadcasting manner. As a result, AP l receives the following signal $\mathbf{Y}_l \in \mathbb{C}^{N \times \tau_p}$:

$$\mathbf{Y}_l = \sum_{k \in \mathcal{K}} \sqrt{p_k} \mathbf{h}_{kl} \phi_{c(k)}^T + \mathbf{N}_l, \quad (4)$$

where p_k is the uplink (UL) transmit power of UE k and $\mathbf{N}_l \in \mathbb{C}^{N \times \tau_p}$ is the receiver noise matrix with i.i.d. elements distributed as $\mathcal{N}_{\mathbb{C}}(0, \sigma^2)$. Then, the l -th AP correlates its

received signal with each pilot available in the pilot pool Φ . The correlation with the t -th pilot yields in

$$\mathbf{y}_{lt} = \mathbf{Y}_l \frac{\phi_t^*}{\|\phi_t\|_2} = \sum_{i \in \mathcal{S}_t} \sqrt{p_i \tau_p} \mathbf{h}_{il} + \mathbf{n}_{lt}, \quad (5)$$

where $\mathbf{n}_{lt} \in \mathbb{C}^N \sim \mathcal{N}_{\mathbb{C}}(\mathbf{0}, \sigma^2 \mathbf{I}_N)$ is the effective receiver noise vector and $\mathcal{S}_t \subset \mathcal{K}$ denotes the set of colliding UEs which chose the same pilot $t \in \mathcal{T}$. Hence, for the t -th pilot, we have that $|\mathcal{S}_t| > 1$ UEs if a collision occurs.

Pilot Activity. On one hand, APs are unable to resolve collisions using the correlated signal \mathbf{y}_{lt} , since they do not have any information about the $|\mathcal{K}|$ UEs. On the other hand, a utility of \mathbf{y}_{lt} is to detect which of the pilots are being used or are active [3]. Locally, the l -th AP can obtain:

$$\frac{1}{N} \|\mathbf{y}_{lt}\|_2^2 \xrightarrow{N \rightarrow \infty} \underbrace{\sum_{i \in \mathcal{S}_t} p_i \tau_p \beta_{il}}_{\alpha_{lt}} + \sigma^2, \quad (6)$$

where $\alpha_{lt} = \sum_{i \in \mathcal{S}_t} p_i \tau_p \beta_{il}$ denotes the UL signal power from the colliding UEs in \mathcal{S}_t regarding pilot $t \in \mathcal{T}$ and AP $l \in \mathcal{L}$. The asymptotic approximation above depends on attaining channel hardening and favorable propagation.¹ A pilot t is said to be an *active pilot* if $\frac{1}{N} \|\mathbf{y}_{lt}\|_2^2 > \sigma^2$. Altogether, AP l knows

$$\tilde{\mathbf{a}}_l \in \mathbb{R}_+^{\tau_p} = \frac{1}{N} [\|\mathbf{y}_{l1}\|_2^2, \|\mathbf{y}_{l2}\|_2^2, \dots, \|\mathbf{y}_{l\tau_p}\|_2^2]^T, \quad (7)$$

where $\tilde{\mathbf{a}}_l$ can be described as the vector that measures pilot activity at AP l . Importantly, we can use $\tilde{\mathbf{a}}_l$ to design a user-centric version of the SUCRe protocol. This can be done by restricting the amount of pilots each AP can serve based on the relative powers stored in $\tilde{\mathbf{a}}_l, \forall l \in \mathcal{L}$. To do this, all L APs send their $\tilde{\mathbf{a}}_l$'s to the CPU. Since τ_p is constant in the order of tens, the communication of τ_p -length vectors $\tilde{\mathbf{a}}_l$'s through fronthaul links is said to be computationally scalable. Then, the CPU knows

$$\tilde{\mathbf{A}} \in \mathbb{R}_+^{\tau_p \times L} = [\tilde{\mathbf{a}}_1, \tilde{\mathbf{a}}_2, \dots, \tilde{\mathbf{a}}_L]. \quad (8)$$

Let $\mathcal{P}_t \subset \mathcal{L}$ denote the subset of APs that attend the t -th pilot ϕ_t for $t \in \mathcal{T}$. The CPU can thus define the APs that will attend pilot t based on the information provided by $\tilde{\mathbf{A}}$. To do so, we suggest the following heuristic procedure:

- 1) Eliminate all *irrelevant* entries of $\tilde{\mathbf{A}}$: set all entries in which $\frac{1}{N} \|\mathbf{y}_{lt}\|_2^2 \leq \sigma^2$ to zero, $\forall l \in \mathcal{L}, \forall t \in \mathcal{T}$.
- 2) Define the maximum number of APs per pilot L^{max} . For simplicity, the integer $1 \leq L^{\text{max}} \leq L$ is assumed to be the same for every pilot $t \in \mathcal{T}$.
- 3) Get the indices of the L^{max} biggest entries of the t -th row of $\tilde{\mathbf{A}}$ that are not irrelevant ones (*i.e.*, not zeros) for each pilot $t \in \mathcal{T}$.
- 4) Construct the subset $\mathcal{P}_t \subset \mathcal{L}$ according to the indices obtained in the previous step for each pilot $t \in \mathcal{T}$.

Each pilot t is then associated to a subset $\mathcal{P}_t \subset \mathcal{L}$ of APs that satisfies $0 \leq |\mathcal{P}_t| \leq L^{\text{max}}$. The t -th pilot is said to be *inactive*

¹We assume that the readers are familiar with channel hardening and favorable propagation concepts. For a more comprehensive definition, we point out the interested reader to [7].

when $|\mathcal{P}_l| = 0$ or $\mathcal{P}_l = \emptyset$. The CPU sends back to the L APs which pilots each AP $l \in \mathcal{L}$ will attend. We let $\mathcal{T}_l \subset \mathcal{T}$ denote the subset of pilots attended by AP l for $l \in \mathcal{L}$. This subset is constructed as $\mathcal{T}_l = \{t : l \in \mathcal{P}_t, \forall t \in \mathcal{T}\}$. The l -th AP can still attend more than one pilot or $0 \leq |\mathcal{T}_l| \leq \tau_p$, where $|\mathcal{T}_l| = 0$ denotes the case in which AP l does not participate in the RA. In the latter case, the l -th AP is said to be *inoperative*.

The physical meaning of \mathcal{P}_t is that it contains the indices of the APs that are closer to the colliding UEs in \mathcal{S}_t . To see this, we seek for a geometric interpretation of \mathcal{P}_t with respect to the distances d_{il} for $i \in \mathcal{S}_t$ and $l \in \mathcal{L}$. From (1), (6), and the inequality $\frac{1}{\sqrt{N}} \|\mathbf{y}_{lt}\|_2^2 > \sigma^2$, the subset \mathcal{P}_t contains the AP indices of the last L^{\max} vector entries:

$$\text{argsort} \left(\left[\sum_{i \in \mathcal{S}_t} p_i d_{i1}^{-\zeta}, \sum_{i \in \mathcal{S}_t} p_i d_{i2}^{-\zeta}, \dots, \sum_{i \in \mathcal{S}_t} p_i d_{iL}^{-\zeta} \right] \right), \quad (9)$$

where the closer an AP $l \in \mathcal{L}$ is to the UEs in \mathcal{S}_t , the greater the sum $\sum_{i \in \mathcal{S}_t} p_i d_{il}^{-\zeta}$. In addition to L^{\max} , another parameter that can change considerably the construction of \mathcal{P}_t 's is the UL transmit power p_i for $i \in \mathcal{S}_t$. However, if all UEs in \mathcal{S}_t transmit with equal power $p_1 = \dots = p_{|\mathcal{S}_t|} = p$, the dependency on p is gone. This means that the construction of \mathcal{P}_t is only controlled by the parameter L^{\max} in this special case, since the other variables are defined by the geometry and environment of a scenario of interest. From the above inequality, one can also note that the subsets C_i and \mathcal{P}_t can be very different for $i \in \mathcal{S}_t$. It is reasonable to expect, however, that $C_i \cap \mathcal{P}_t \neq \emptyset$ for most of the colliding UEs $i \in \mathcal{S}_t$. The intuition behind this expectation is because \mathcal{P}_t depends on $\sum_{i \in \mathcal{S}_t} p_i \tau_p \beta_{il}$, while C_i on the individual $q_l \beta_{il}$'s for $i \in \mathcal{S}_t$. Both quantities are positively correlated to the magnitude of average channel gains β_{il} for $i \in \mathcal{S}_t$ and $l \in \mathcal{L}$.

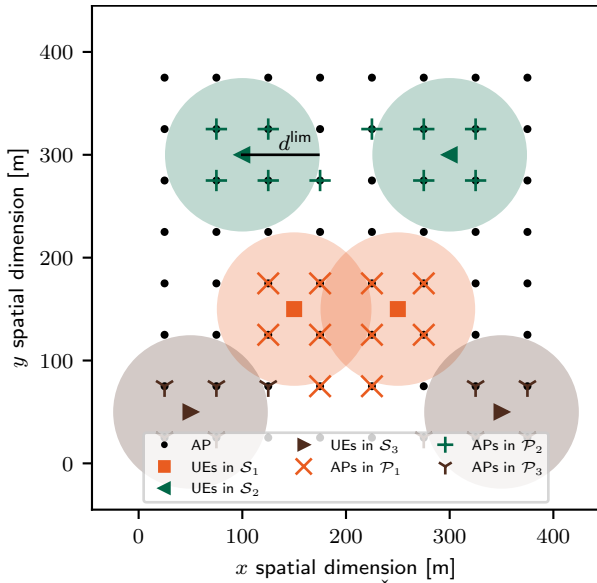


Fig. 2. Illustrative construction of the subsets \check{C}_k and \mathcal{P}_t for $L^{\max} = 10$ APs. There are $L = 64$ APs disposed in an 8×8 square grid over a coverage area of $400 \text{ m} \times 400 \text{ m}$. Each color represents a pilot $t \in \mathcal{T} = \{1, 2, 3\}$. Each pilot has $|\mathcal{S}_t| = 2$ UEs colliding in different spatial arrangements: \mathcal{S}_1 '■', \mathcal{S}_2 '▲', and \mathcal{S}_3 '▶'. The colored circles with radius $d^{\text{lim}} \approx 73.30 \text{ m}$ mark the UE's influence region. The APs '•' within of the colored circles are in \check{C}_k for $k \in \mathcal{S}_t$. APs with different markers superimposed over '•' indicates the construction of \mathcal{P}_1 , \mathcal{P}_2 , and \mathcal{P}_3 . Fixed parameters are: $\Omega = -30.5 \text{ dB}$, $\zeta = 3.67$, $\sigma^2 = -94 \text{ dBm}$, $\tau_p = 3$, $p = 100 \text{ mW}$, and $q_l = 200/64 \text{ mW}$.

Fig. 2 illustrates the process of obtaining subsets \check{C}_k and \mathcal{P}_t for $L^{\max} = 10$ APs. For illustrative reasons, we consider that the asymptotic approximation in (6) is obtained. There are $\tau_p = 3$ active pilots, where for each pilot a collision of size $|\mathcal{S}_t| = 2$ UEs occurs. This gives rise to the colliding sets: \mathcal{S}_1 '■', \mathcal{S}_2 '▲', and \mathcal{S}_3 '▶'. These markers denote the positions of the UEs. The APs that comprise the natural subset \check{C}_k of each UE $i \in \mathcal{S}_t$ are the ones within the UE's influence region delimited by the colored circles of radius d^{lim} , which is calculated according to (3). The subset of APs attending each one of the pilots $\mathcal{P}_1, \mathcal{P}_2, \mathcal{P}_3$ are also differentiated by markers. From the figure, it can be noted that \mathcal{P}_t does not necessarily match perfectly with \check{C}_k for $k \in \mathcal{S}_t$ and given a L^{\max} . The main goal of limiting the number $|\mathcal{P}_t|$ of APs that are attending each pilot is to mitigate the computational complexity and the inter-AP interference that could arise. As a result, the CF-SUCRe protocol can become more energy efficient, since not all L APs necessarily operate in the RA.

C. Step 2: Precoded RA Response

Let $\mathcal{P} = \cup_{t=1}^{\tau_p} \mathcal{P}_t$ denote all the APs that attend at least one pilot $t \in \mathcal{T}$. AP $l \in \mathcal{P}$ sends the following precoded DL pilot signal $\mathbf{V}_l \in \mathbb{C}^{N \times \tau_p}$ employing a multi-cast maximum-ratio (MR) transmission:

$$\mathbf{V}_l = \sqrt{q_l} \sum_{t \in \mathcal{T}_l} \frac{\mathbf{y}_{lt}}{\|\mathbf{y}_{lt}\|_2} \phi_t^T, \quad (10)$$

where q_l is the transmit power per pilot t of AP l . Note that the MR precoding vector $\mathbf{y}_{lt}/\|\mathbf{y}_{lt}\|_2$ spatially directs the t -th pilot towards the colliding UEs in \mathcal{S}_t . The received signal $\mathbf{z}_k \in \mathbb{C}^{\tau_p}$ at UE $k \in \mathcal{S}_t$ is then:

$$\mathbf{z}_k^T = \sum_{l \in \mathcal{P}} \mathbf{h}_{kl}^H \mathbf{V}_l + \boldsymbol{\eta}_k^T, \quad (11)$$

where $\boldsymbol{\eta}_k \sim \mathcal{N}_{\mathbb{C}}(\mathbf{0}, \sigma^2 \mathbf{I}_{\tau_p})$ is the receiver noise. The k -th UE correlates \mathbf{z}_k^T with the pilot ϕ_t used in Step 1, yielding in:

$$\begin{aligned} z_k &= \mathbf{z}_k^T \frac{\phi_t^*}{\|\phi_t\|_2} = \sum_{l \in \mathcal{P}_t} \sqrt{q_l \tau_p} \mathbf{h}_{kl}^H \frac{\mathbf{y}_{lt}}{\|\mathbf{y}_{lt}\|_2} + \eta_{kt}, \\ &\stackrel{(a)}{=} \underbrace{\sum_{l \in \mathcal{P}_t} \sqrt{\frac{q_l p_k \tau_p^2}{\|\mathbf{y}_{lt}\|_2^2}} \|\mathbf{h}_{kl}\|_2^2}_{\text{effective channel}} + \underbrace{\sum_{i \in \mathcal{S}_t \setminus \{k\}} \left(\sum_{l \in \mathcal{P}_t} \sqrt{\frac{q_l p_i \tau_p^2}{\|\mathbf{y}_{lt}\|_2^2}} \mathbf{h}_{kl}^H \mathbf{h}_{il} \right)}_{\text{effective interfering channel}} \\ &\quad + \underbrace{\sum_{l \in \mathcal{P}_t} \sqrt{\frac{q_l \tau_p}{\|\mathbf{y}_{lt}\|_2^2}} \mathbf{h}_{kl}^H \mathbf{n}_{lt}}_{\text{noise}} + \eta_{kt}, \end{aligned} \quad (12)$$

where in (a) we used (5) and $\eta_{kt} \sim \mathcal{N}_{\mathbb{C}}(0, \sigma^2)$ is the effective receiver noise. Based on the channel hardening property [7], the effective channel above can satisfy

$$\begin{aligned} &\frac{1}{\sqrt{N}} \sum_{l \in \mathcal{P}_t} \sqrt{\frac{q_l p_k \tau_p^2}{\|\mathbf{y}_{lt}\|_2^2}} \|\mathbf{h}_{kl}\|_2^2 - \\ &-\frac{1}{\sqrt{N}} \left(\mathbb{E} \left\{ \sum_{l \in \mathcal{P}_t} \sqrt{\frac{q_l p_k \tau_p^2}{\|\mathbf{y}_{lt}\|_2^2}} \|\mathbf{h}_{kl}\|_2^2 \right\} \right) \rightarrow 0, \text{ as } N \rightarrow \infty. \end{aligned} \quad (13)$$

Hence, if favorable propagation also holds, we have the following approximation $\tilde{z}_k \in \mathbb{R}_+$ using the principles of the law of large numbers:

$$\frac{\Re(z_k)}{\sqrt{N}} \approx \tilde{z}_k = \sum_{l \in \mathcal{P}_t} \left(\frac{\sqrt{q_l} p_k \tau_p \beta_{kl}}{\sqrt{\alpha_{lt} + \sigma^2}} \right), \quad (14)$$

where $\Re(z_k)$ stands for the real part of $z_k \in \mathbb{C}$ and α_{lt} was defined in (6). The guess \tilde{z}_k in (14) is handy for UE $k \in \mathcal{S}_t$ to provide a way to compare its total UL signal power $\gamma_k \in \mathbb{R}_+$:

$$\gamma_k = \sum_{l' \in \mathcal{C}_k} p_k \tau_p \beta_{kl'} \quad (15)$$

with the total UL signal power $\alpha_t \in \mathbb{R}_+$ from the colliding UEs in \mathcal{S}_t :

$$\alpha_t = \sum_{l \in \mathcal{P}_t} \alpha_{lt} = \sum_{i \in \mathcal{S}_t} \left(\sum_{l \in \mathcal{P}_t} p_l \tau_p \beta_{il} \right), \quad (16)$$

where we used the definition of α_{lt} in (6). It is worth noting that UE k knows γ_k , whereas α_t is unknown to UE k . The key idea behind SUCRe introduced in [3] is to resolve the collision by having the strongest UE among those $|\mathcal{S}_t|$ colliding re-transmitting the t -th pilot. In order for UE k to be able to determine if he is the strongest UE, he needs to estimate α_t having the correlated received signal z_k in (12) as information. We will denote any estimation of α_t by UE $k \in \mathcal{S}_t$ as $\hat{\alpha}_{t,k}$. In Section IV, we discuss different estimators for $\hat{\alpha}_{t,k}$.

D. Step 3: Collision Resolution & Pilot Repetition

In this step, each UE solves the pilot collision through a distributed process called as *collision or contention resolution*. Based on SUCRe [3] and considering the asymptotic case of $N \rightarrow \infty$, each UE $k \in \mathcal{K}$ applies the following distributed rule to decide whether it is the contention winner or not:

$$\begin{aligned} R_k : \gamma_k &> \frac{\hat{\alpha}_{t,k}}{2} \text{ (repeat),} \\ I_k : \gamma_k &\leq \frac{\hat{\alpha}_{t,k}}{2} \text{ (inactive),} \end{aligned} \quad (17)$$

where $\hat{\alpha}_{t,k}$ denotes any estimation of α_t made by UE k . This *distributed decision rule* reads as follows: UE $k \in \mathcal{S}_t$ re-transmits the pilot signal ϕ_t if and only if it has its own total UL signal power γ_k greater than half of the estimated total UL signal power $\hat{\alpha}_{t,k}$ from all the colliding UEs in $i \in \mathcal{S}_t$, and hypothesis R_k is therefore true; otherwise, if UE k concludes that hypothesis I_k is true, it decides to pull out of and postpone the access attempt. Here, different from [3], we consider that there are no bias parameters to tune the decision rule. Step 3 finishes with the re-transmission of the same pilots sent in Step 1 by the UEs that have decided for R_k .

E. Step 4: Allocation of Dedicated Data Payload Pilots

The L APs receive the pilots repeated by the winning contention UEs. The l -th AP only needs to check the re-transmitted pilots that are served by it, which are specified by $\mathcal{T}_l \subset \mathcal{T}$ for $l \in \mathcal{L}$. An important difference of the CF-SUCRe compared to the cellular version is that two or more UEs can

consider themselves contention winners and yet the two or more UEs can still join the network. To see this, we consider the following example exploring what we call the concept of *spatial separability* arising from the macro-diversity of cell-free systems.

Example. (Two Colliding UEs) *Let us assume the case of two colliding UEs in $\mathcal{S}_t = \{1, 2\}$. Both UEs consider themselves winners of the contention, transmitting pilot t back in Step 3. Given a suitable choice of L^{\max} , the colliding UEs \mathcal{S}_t are served by the subset \mathcal{P}_t of APs. By checking $(\mathcal{P}_t \cap \check{\mathcal{C}}_1) \setminus (\mathcal{P}_t \cap \check{\mathcal{C}}_2)$ and vice-versa, it is possible to see if some of the APs in \mathcal{P}_t are only close to one of the two colliding UEs. If that is the case, it is reasonable to assume that those APs that are only close to one of the UEs are still able to spatially separate that UE, seeing that the interference from the re-transmission of the other UE is low due to the increased distance. Fig. 3 illustrates the discussed concept called *spatial separability*. Hence, when two colliding UEs re-transmit in Step 3, there can be: the acceptance of both, the acceptance of one of the two, or the acceptance of neither, depending on the subsets $\check{\mathcal{C}}_i$ and \mathcal{P}_t for $i \in \mathcal{S}_t$.*

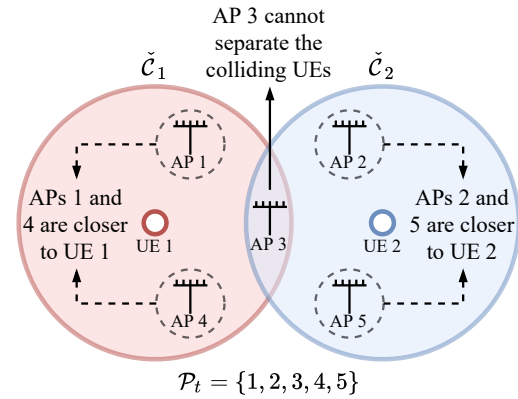


Fig. 3. Illustration of the concept of spatial separability when considering a set of two colliding UEs $\mathcal{S}_t = \{1, 2\}$ served by five APs in $\mathcal{P}_t = \{1, 2, 3, 4, 5\}$.

The concept of spatial separability is generalized in Algorithm 1. The intuition behind the algorithm is to find APs in \mathcal{P}_t that are particular to a single UE $k \in \mathcal{S}_t$. It is worthwhile to note the use of the natural subsets $\check{\mathcal{C}}_i$ so that one can guarantee that the inter-UE interference is negligible for $i \in \mathcal{S}_t$. The APs that are able to spatially separate a UE can estimate its channel and successfully decode the messages used to finally establish its connection to the network.

IV. ESTIMATING TOTAL UL SIGNAL POWER FROM COLLIDING UES

In this section, we introduce three different methods to estimate the total UL signal power α_t from the colliding UEs in \mathcal{S}_t for UE $k \in \mathcal{S}_t$. Recall that the estimate of α_t is used in such a way as to allow UEs to perform the SUCRe process defined in eq. (17) from Step 3.

A. Estimator 1

The first method is based on the simplifying assumption that the different signal powers α_{lt} 's for $l \in \mathcal{P}_t$ are almost equal.

Algorithm 1 Determining spatial separability.

1: **Input:** Set of colliding UEs: \mathcal{S}_t ; Natural subset of APs known by UE $i \in \mathcal{S}_t$: $\check{\mathcal{C}}_i$; Set of APs attending pilot t : \mathcal{P}_t ; Binary set of decisions of all colliding UEs:

$$\mathcal{E}_t = \{d : d = 0, \text{ if } i \text{ decided } I_i, d = 1, \text{ o/w, } i \in \mathcal{S}_t\}.$$

2: **Output:** # of successful attempts $s \in \{0, 1, \dots, |\mathcal{S}_t|\}$.

3: **Procedure:**

4: **if** $|\mathcal{E}_t \cap \{0\}| == |\mathcal{S}_t|$ **then** \triangleright none UE $i \in \mathcal{S}_t$ re-transmitted

5: **return** $s \leftarrow 0$

6: **end if**

7: **if** $|\mathcal{E}_t \cap \{1\}| == 1$ **then** \triangleright only a UE $i \in \mathcal{S}_t$ re-transmitted

8: **return** $s \leftarrow 1$

9: **end if**

10: **for** $k \in \mathcal{S}_t$ **do** \triangleright more than one UE $i \in \mathcal{S}_t$ re-transmitted

11: $\check{\mathcal{C}}_k = \bigcup_{i \in \mathcal{S}_t \setminus \{k\}} \check{\mathcal{C}}_i$

12: **if** $\mathcal{P}_t \cap \check{\mathcal{C}}_k \neq \emptyset$ **and** $(\mathcal{P}_t \cap \check{\mathcal{C}}_k) \setminus (\mathcal{P}_t \cap \check{\mathcal{C}}_k) \neq \emptyset$ **then**

\triangleright check if UE $k \in \mathcal{S}_t$ is *spatially separable*

13: $s \leftarrow s + 1$

14: **end if**

15: **end for**

16: **return** s

Therefore, we can assume that α_{lt} in (14) is independent of the AP index l , yielding the following estimate:

$$\hat{\alpha}_{t,k}^{\text{est1}} = N \left(\frac{\sum_{l \in \mathcal{P}_t} \sqrt{q_l p_k} \tau_p \beta_{kl}}{\mathfrak{R}(z_k)} \right)^2 - \sigma^2. \quad (18)$$

However, this estimator is unfeasible because the k -th UE does not know \mathcal{P}_t . Since UE k only knows the average channel gains towards the APs in \mathcal{C}_k and it is reasonable to expect that $\mathcal{P}_t \cap \mathcal{C}_k \neq \emptyset$, a heuristic way to turn the above estimator into a feasible one is to approximate it as:

$$\hat{\alpha}_{t,k}^{\text{est1,approx}} = N \left(\frac{\sum_{l' \in \mathcal{C}_k} \sqrt{q_{l'} p_k} \tau_p \beta_{kl'}}{\mathfrak{R}(z_k)} \right)^2 - \sigma^2. \quad (19)$$

Note that the summation is realized now over \mathcal{C}_k . Together with this first approximation, we can use the fact that the k -th UE approximately knows part of its own contribution to the estimate $\hat{\alpha}_{t,k}^{\text{est1,approx}}$, which is given by γ_k defined in (15). Therefore, the first estimator for α_t in (16) is

$$\hat{\alpha}_{t,k}^{\text{est1,approx}} = \max \left(N \left(\frac{\sum_{l' \in \mathcal{C}_k} \sqrt{q_{l'} p_k} \tau_p \beta_{kl'}}{\mathfrak{R}(z_k)} \right)^2 - \sigma^2, \gamma_k \right). \quad (20)$$

Using γ_k avoids overly underestimation, since the estimate must be at least in the same order of magnitude of γ_k .

In addition to \tilde{z}_k in (14), Estimator 1 relies on two other approximations. First, due to the simplifying hypothesis of equal α_{lt} 's for $l \in \mathcal{P}_t$, the following condition must be satisfied by the APs in \mathcal{P}_t :

$$\underbrace{\sum_{i \in \mathcal{S}_t} \beta_{i1}}_{\text{AP 1}} = \underbrace{\sum_{i \in \mathcal{S}_t} \beta_{i2}}_{\text{AP 2}} = \dots = \underbrace{\sum_{i \in \mathcal{S}_t} \beta_{i|\mathcal{P}_t|}}_{\text{AP } |\mathcal{P}_t|}. \quad (21)$$

Geometrically, this means that, if the colliding UEs transmit with the same UL power p , the APs must have the same aggregated effective distances $\sum_{i \in \mathcal{S}_t} d_{il}^{-\zeta}$ to the colliding UEs for $l \in \mathcal{P}_t$, as can be inferred from (9). Intuitively, note that this condition is easier to be satisfied when $|\mathcal{P}_t|$ is small. Hence, it is expected that this estimator will work better for small collision sizes $|\mathcal{S}_t|$, which requires smaller number of APs attending pilot t . Second, due to the approximation of \mathcal{P}_t by \mathcal{C}_k on the UE's side, the following sums need to have the same order of magnitude:

$$\sum_{l \in \mathcal{P}_t} \sqrt{q_l p_k} \tau_p \beta_{kl} \approx \sum_{l' \in \mathcal{C}_k} \sqrt{q_{l'} p_k} \tau_p \beta_{kl'} \rightarrow \sum_{l \in \mathcal{P}_t} \beta_{kl} \approx \sum_{l' \in \mathcal{C}_k} \beta_{kl'}.$$

The problem occurs when the scaling of the sums are not compatible, due to the intrinsic difference between the two subsets of APs, deteriorating estimation performance.

B. Estimator 2

The second method avoids the simplifying assumption made in Estimator 1 of equal α_{lt} 's and relies on solving the following optimization problem:

$$\begin{aligned} \underset{\alpha_t \in \mathbb{R}_+^{|\mathcal{P}_t|}}{\text{argmin}} \quad & f(\alpha_t) = \|\alpha_t\|_1 = \sum_{l \in \mathcal{P}_t} \alpha_{lt}, \\ \text{s.t.} \quad & g(\alpha_t) = \frac{\mathfrak{R}(z_k)}{\sqrt{N}} - \tilde{z}_k(\alpha_t) = 0, \end{aligned} \quad (22)$$

where α_{lt} 's for $l \in \mathcal{P}_t$ are organized in vector form as $\alpha_t \in \mathbb{R}_+^{|\mathcal{P}_t|} = [\alpha_{1t}, \alpha_{2t}, \dots, \alpha_{|\mathcal{P}_t|t}]^\top$ and $\tilde{z}_k(\alpha_t)$ shows dependence of the approximation with α_t . Moreover, $f(\alpha_t) : \mathbb{R}_+^{|\mathcal{P}_t|} \mapsto \mathbb{R}_+$ is a linear objective function and $g(\alpha_t) : \mathbb{R}_+^{|\mathcal{P}_t|} \mapsto \mathbb{R}_+$ is a non-linear equality constraint. The motivation behind formulating the problem above comes from the experimental observation that the approximation \tilde{z}_k often overestimates the true value $\mathfrak{R}(z_k)/\sqrt{N}$. In general, this means that most likely $\tilde{z}_k \geq \mathfrak{R}(z_k)/\sqrt{N}$, implying that $g(\alpha_t) < 0$ for finite, small N . The problem in (22) is thus a way to combat this overestimation of \tilde{z}_k by finding the vector α_t which minimizes the total UL signal power α_t from the colliding UEs given that the constraint is supposedly satisfied. The result below gives a closed-form solution for (22) using the method of Lagrange multipliers and considering all involved quantities as deterministic.

Theorem 1. Let $\hat{\alpha}_{t,k}^{\text{est2}}$ denote the estimate of α_{lt} made by UE $k \in \mathcal{S}_t$. Using the approximation in (14), we get that:

$$\hat{\alpha}_{t,k}^{\text{est2}} = N \left(\frac{\sum_{l' \in \mathcal{P}_t} (\sqrt{q_{l'} p_k} \tau_p \beta_{kl'})^{2/3}}{\mathfrak{R}(z_k)} \right)^2 (\sqrt{q_l p_k} \tau_p \beta_{kl})^{2/3} - \sigma^2, \quad (23)$$

for all $l \in \mathcal{P}_t$. Therefore, $\hat{\alpha}_{t,k}^{\text{est2}} = \sum_{l \in \mathcal{P}_t} \hat{\alpha}_{t,k}^{\text{est2}}$.

Proof. The proof can be seen in the Appendix. \square

However, as in the case of Estimator 1, the estimate obtained in Theorem 1 is unfeasible due to the fact that \mathcal{P}_t is unknown to UE $k \in \mathcal{S}_t$. As before, we assume that the best guess that

UE k can obtain is to perform the estimation over the subset C_k of known APs. This results in

$$\hat{\alpha}_{t,k}^{\text{est2,approx}} = N \left(\frac{\sum_{l' \in C_k} \text{cte}_{kl'}}{\mathfrak{R}(z_k)} \right)^2 (\text{cte}_{kl})^{2/3} - \sigma^2,$$

for all $l \in C_k$ and where $\text{cte}_{kl} = \sqrt{q_l p_k} \tau_p \beta_{kl}$. Therefore,

$$\hat{\alpha}_{t,k}^{\text{est2,approx}} = \max \left(\hat{\alpha}_{t,k}^{\text{est2,approx}}, \gamma_k \right), \quad (24)$$

where $\hat{\alpha}_{t,k}^{\text{est2,approx}} = \sum_{l' \in C_k} \hat{\alpha}_{l',k}^{\text{est2,approx}}$. Different from Estimator 1 that relies on two approximations other than \tilde{z}_k , Estimator 2 is based only in approximating the sum of the average channel gains over \mathcal{P}_t by C_k .

C. Estimator 3

The third estimator relies on taking more advantage of the fact that the CPU knows the pilot activity matrix $\tilde{\mathbf{A}}$. From this information and the expression in (6), the CPU can obtain an estimate of the total UL signal power from colliding UEs:

$$\hat{\alpha}_t = \sum_{l \in \mathcal{L}} \max \left(\tilde{a}_{tl} - \sigma^2, 0 \right) = \sum_{l \in \mathcal{L}} \max \left(\frac{1}{N} \|\mathbf{y}_{tl}\|_2^2 - \sigma^2, 0 \right), \quad (25)$$

where \tilde{a}_{tl} is entry (t, l) of $\tilde{\mathbf{A}}$. Then, this estimate can be sent back to the APs in \mathcal{P}_t that attend the t -th pilot and the DL precoded signal in (10) can be re-designed as:

$$\mathbf{V}_t = \sqrt{q_t} \sum_{l \in \mathcal{P}_t} \frac{\mathbf{y}_{tl}}{\sqrt{N \cdot \hat{\alpha}_t}} \boldsymbol{\phi}_t^T. \quad (26)$$

Its effective DL transmit power \tilde{q}_{tl} per pilot t of AP l is

$$\tilde{q}_{tl} = \left(\frac{q_l}{N \cdot \hat{\alpha}_t} \right) \|\mathbf{y}_{tl}\|_2^2. \quad (27)$$

When analyzing \tilde{q}_{tl} , it is natural to expect that APs will transmit with less power when adopting the precoding in (26) than that in (10). With the DL precoded signal in (26), the approximation \tilde{z}_k becomes:

$$\frac{\mathfrak{R}(z_k)}{\sqrt{N}} \approx \tilde{z}_k = \sum_{l \in \mathcal{P}_t} \left(\frac{\sqrt{q_l p_k} \tau_p \beta_{kl}}{\sqrt{\hat{\alpha}_t}} \right) = \frac{1}{\sqrt{\hat{\alpha}_t}} \sum_{l \in \mathcal{P}_t} \sqrt{q_l p_k} \tau_p \beta_{kl}. \quad (28)$$

The k -th UE can combat the low received power in z_k due to (27) by multiplying the received signal z_k by a *compensation factor* δ . This pre-processing operation can be described as:

$$\underline{\mathfrak{R}}(z_k) = \delta \left(\frac{\mathfrak{R}(z_k) - \sigma}{\sqrt{N}} \right), \quad (29)$$

whose subtraction by σ helps in not increasing the magnitude of the noise by a factor of δ .² A trivial estimator of α_t is then:

$$\hat{\alpha}_{t,k}^{\text{est3,approx}} = \max \left(N \left(\frac{\sum_{l' \in C_k} \sqrt{q_{l'} p_k} \tau_p \beta_{kl'}}{\underline{\mathfrak{R}}(z_k)} \right)^2, \gamma_k \right), \quad (30)$$

which also adopts the approximation of substituting \mathcal{P}_t by C_k . The main difference between Estimator 1 and Estimator 3 is that now the α_{tl} 's are in fact equal by construction of the DL

²Although the compensation factor coherently multiplies a part of the interference and noise components, this method provides gain in terms of energy efficiency as the APs transmit with less power.

precoded signal, because the latter uses the common factor $(N \cdot \hat{\alpha}_t)^{-1/2}$ in (26) to normalize the precoded DL signal of all APs in \mathcal{P}_t . Moreover, the compensation factor δ helps to decrease the amount of APs in \mathcal{P}_t that need to be operative to attend pilot t so as to obtain a reasonable estimation performance. In fact, due to the low transmit power of the DL precoded signal in (26), it is intuitive that more APs are needed in \mathcal{P}_t to serve the colliding UEs in \mathcal{S}_t if the compensation factor δ is not used by these UEs. One way to obtain such δ is to find and characterize the following ratio:

$$\delta = \sqrt{\frac{q_l}{\tilde{q}_l^{\text{avg}}}}, \quad (31)$$

where \tilde{q}_l^{avg} is the average of \tilde{q}_{tl} defined in (27) with respect to the number of active pilots, number of operative APs, and channel realizations given a number of inactive users $|\mathcal{U}|$ and probability of activation P_a . Below, we characterize how and when the UEs can obtain such information and a suitable value of δ for a scenario of interest.

Remark 1. (Comparison with Ce-SUCRe) *Interestingly, all estimators have a similar expression when considering the cellular case where $L = 1$ AP and $N = M$ antennas. In this particular case, the estimators become the same as the first estimation method proposed in [3]:*

$$\hat{\alpha}_{t,k}^{\text{est,approx}} = \max \left(\frac{M q p_k \tau_p^2 \beta_k^2}{(\mathfrak{R}(z_k))^2} - \sigma^2, p_k \tau_p \beta_k \right). \quad (32)$$

This suggests that our CF-SUCRe protocol can be seen as a generalization of the Ce-SUCRe by [3], where a BS equipped with M antennas serves the set of inactive UEs \mathcal{U} .

Remark 2. (Estimators' Dependency with ι and L^{\max}) *All estimators rely on the approximation of \mathcal{P}_t by C_k . This therefore means that the performance of the estimators also depends on the choice of the parameters ι and L^{\max} , since they control the sizes $|C_k|$ and $|\mathcal{P}_t|$, respectively.*

D. Numerically Evaluating Estimators

In this part, we are interested in better understanding how the three estimators proposed above operate. To do this, we consider a square coverage area of 400 m \times 400 m. This area is served by a cell-free mMIMO network comprised of $L = 64$ APs disposed in an 8 \times 8 square grid layout, as illustrated in Fig. 2. Each AP is equipped with $N = 8$ antennas, unless stated otherwise. We fix the number of antennas N per AP in such a way as to obtain a reasonable approximation \tilde{z}_k in (14). Other simulation parameters are summarized in Table I. Note that we assume that UEs transmit with equal power p . We evaluate the performance of the estimators through the use of two metrics regarding UE $k \in \mathcal{S}_t$, which are defined as: **i)** *normalized estimation bias* (NEB) $b_{t,k} = (\mathbb{E}\{\hat{\alpha}_{t,k}\} - \alpha_t) / \alpha_t$; and **ii)** *normalized mean squared error* (NMSE) $\text{NMSE}_{t,k} = \mathbb{E}\{|\hat{\alpha}_{t,k} - \alpha_t|^2\} / \alpha_t^2$. The expectations are taken with respect to channel realizations.

1) *Evaluating Approximation of \mathcal{P}_t by C_k :* In Fig. 4, we particularly evaluate the approximation $\sum_{l \in \mathcal{P}_t} \beta_{kl} \approx$

TABLE I
SIMULATION PARAMETERS

Parameter	Value
multiplicative power constant Ω	-30.5 dB
pathloss exponent ζ	3.67
noise power σ^2	-94 dBm
# of pilots τ_p	5
# of APs L	64 APs
# of antennas per AP N	8
DL transmit power per AP q_l	200/64 mW
UL transmit power p	100 mW
# of BS antennas M	64
DL transmit power of BS q	200 mW
# of setups	100
# of channel realizations	100

$\sum_{l' \in C_k} \beta_{kl'}$ that makes the proposed estimators viable for $C_k = \check{C}_k$. The *normalized magnitude difference* (NMD) is defined as

$$\text{NMD}_k = \left(\sum_{l \in \mathcal{P}_t} \beta_{kl} - \sum_{l' \in \check{C}_k} \beta_{kl'} \right) / \sum_{l \in \mathcal{P}_t} \beta_{kl}, \quad \text{for UE } k \in \mathcal{S}_t.$$

The average NMD, denoted as $\overline{\text{NMD}}$, is obtained by averaging out the NMD_k from colliding UEs in \mathcal{S}_t and several realizations of \mathcal{S}_t . From Fig. 4a, we can see that the difference in the scale of the sums is more substantial for small L^{\max} . The intuition behind this result is that, for small L^{\max} , some of the APs contained in \check{C}_k will not be selected in the construction of \mathcal{P}_t . One way to reduce this effect is to vary the size of C_k instead of using \check{C}_k , as better evaluated in the following analysis. The trend in Fig. 4b reveals other important insights. First, it is possible to verify again that the larger the collision size $|\mathcal{S}_t|$ and the smaller the L^{\max} , the more likely that $\beta_{kl'}$ of large magnitudes (most important APs) for the colliding UEs $k \in \mathcal{S}_t$ will be excluded when constructing \mathcal{P}_t , since it is more probable that $\sum_{l \in \mathcal{P}_t} \beta_{kl} < \sum_{l' \in \check{C}_k} \beta_{kl'}$. Second, for a value of L^{\max} large enough, the opposite is true: it becomes more likely that $\sum_{l \in \mathcal{P}_t} \beta_{kl} > \sum_{l' \in \check{C}_k} \beta_{kl'}$. For example, this condition is illustrated in Fig. 2. However, the larger the collision size $|\mathcal{S}_t|$, the more unlikely it is to attain the condition $\sum_{l \in \mathcal{P}_t} \beta_{kl} > \sum_{l' \in \check{C}_k} \beta_{kl'}$. This is because the APs closest to a UE k are included in $C_k \subset \mathcal{P}_t$ for increasing L^{\max} , while the other APs in $(\mathcal{P}_t \setminus C_k) \cap \mathcal{P}_t$ have average channel gains β_{kl} of decreasing magnitude w.r.t. the k -th UE due to increasing distance. Third, Fig. 4 uncovers the importance of selecting L^{\max} . This parameter must be selected carefully such that the probability $\mathbb{P}\{\sum_{l \in \mathcal{P}_t} \beta_{kl} > \sum_{l' \in \check{C}_k} \beta_{kl'}\}$ is close to 50%, meaning that $\sum_{l \in \mathcal{P}_t} \beta_{kl} \approx \sum_{l' \in \check{C}_k} \beta_{kl'}$.

2) *Estimator 3 differences*: We now want to understand how the effective DL transmit power \tilde{q}_{lt} in (27) of the framework used to obtain Estimator 3 changes compared to the more traditional method of transmission defined in (10). The latter has a DL transmit power per pilot of q_l . By varying the collision sizes $|\mathcal{S}_t|$ from 1 to 10, UEs' positions, and channel realizations, we found that \tilde{q}_{lt} has an average value of approximately $\tilde{q}_{lt}^{\text{avg}} = 0.0489$ mW for $L^{\max} = 64$ APs. When

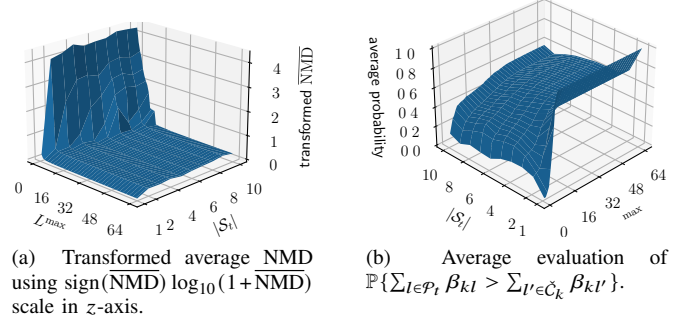


Fig. 4. Evaluation of the approximation $\sum_{l \in \mathcal{P}_t} \beta_{kl} \approx \sum_{l' \in \check{C}_k} \beta_{kl'}$ for different collision sizes $|\mathcal{S}_t|$ and choices of L^{\max} .

compared to the value of $q_l = 200/64 = 3.125$ mW, it is possible to certify that the power of the precoding used in (26) is extremely reduced. For the defined simulation setting, the compensation factor is approximately $\delta \approx 8$. We will use this value below to evaluate Estimator 3. In Subsection IV-E, we discuss how the APs can estimate δ and share this information with all $|\mathcal{U}|$ inactive UEs.

3) *General performance comparison*: Our goal here is to observe **i)** how the performance of the estimators behave under different collision sizes $|\mathcal{S}_t|$ and **ii)** how the choice of the parameter pair (ι, L^{\max}) affects the performance of each estimator, following the observation made in Remark 2. To evaluate how the estimators perform for increasing collision size $|\mathcal{S}_t|$, we propose the following simulation routine: **1) Setup**: a setup is generated by fixing the number of colliding UEs $|\mathcal{S}_t|$ and by dropping these $|\mathcal{S}_t|$ UEs over the coverage area at random; **2) Channel Realizations**: several channel realizations are generated for the created setup in 1). For each estimator, we obtain the $\text{NMSE}_{t,k}$ of every UE k in \mathcal{S}_t and store them; **3) Statistics**: after the realization of several setups, we evaluate the median value of the stored $\text{NMSE}_{t,k}$'s together with their interquartile range (IQR), which evaluates the statistical dispersion of the values by subtracting the lower and upper quartiles. This procedure is evaluated for all combinations of (ι, L^{\max}) within a suitable range. For simplicity, instead of varying ι , we actually parameterize its variation by directly adjusting the size $|C_k|$ of known APs by UE $k \in \mathcal{S}_t$. Moreover, we ensure that $|C_k|$ can never be larger than $|\check{C}_k|$. Therefore, for the considered parameters and geometry, an appropriate range for $|C_k| \in \{1, 2, \dots, 7\}$ and for $L^{\max} \in \mathcal{L}$, as can be inferred from Fig. 2.

First, after the realization of the aforementioned procedure, we seek for the best pair of parameters $(|C_k|, L^{\max})$ in the sense of obtaining the smallest median NMSE for each one of the evaluated collision sizes $|\mathcal{S}_t|$ and proposed estimators. We report the best parameter pairs $(|C_k|, L^{\max})$ in Table II. As expected, by increasing the number of colliding UEs in $\mathcal{S}_t > 1$, one can observe that it is necessary to increase the number of APs $|\mathcal{P}_t|$ or L^{\max} that serve those UEs in order to improve the performance of the estimators. We also notice that the optimal median value of $|C_k|$ that allows a better approximation of $\sum_{l \in \mathcal{P}_t} \beta_{kl} \approx \sum_{l' \in C_k} \beta_{kl'}$ does not vary so much.

Fig. 5 shows the best median NMSE obtained for each one

TABLE II
BEST PARAMETER PAIR ($|C_k|, L^{\max}$) AT MEDIAN FOR DIFFERENT COLLISION SIZES AND $N = 8$ ANTENNAS PER AP

Collision size $ S_t $	1	2	3	4	5	6	7	8	9	10
Est. 1	(6,6)	(7,4)	(5,4)	(5,5)	(7,7)	(5,9)	(7,10)	(6,10)	(7,11)	(6,12)
Est. 2	(6,9)	(7,7)	(7,7)	(6,7)	(6,7)	(7,8)	(7,9)	(7,10)	(7,12)	(7,11)
Est. 3	(1,1)	(7,3)	(7,4)	(7,7)	(7,8)	(7,10)	(6,11)	(7,10)	(6,11)	(7,12)

of the estimators when adopting the pairs of parameters shown in Table II. As a baseline, we consider a cellular mMIMO network in which a cell-centered BS equipped with $M = 64$ antennas serves the colliding UEs; the estimator stated in Remark 1 is used in such situation. Furthermore, in an attempt to be fair in the comparison between the cellular and cell-free cases, the DL transmit power of the BS is $q = L \cdot q_l$, in such a way as to have the same amount of power in the entire coverage area $\sum_{l=1}^L q_l = q = 200$ mW for both networks. The other parameters of the cellular case follows the ones stated in Table I. The results presented in the figure reveal, at median, that among the three cell-free estimators: a) Estimator 3 is the best in the case of no collision $|S_t| = 1$, b) Estimator 2 works better than the other two on almost all collision sizes. Another interesting fact to note is that the cell-free estimators perform better than the cellular case on almost all evaluated scenarios. The intuition behind this result is the geographic arrangement of APs, which can eventually help to mitigate the bad effect of collisions since UEs tend to be far away and the APs around them are therefore distinct; that is, they have distinct C_k 's. Furthermore, \mathcal{P}_t is constructed in such a way that there are APs near each one of the colliding UEs. As a consequence, we have to increase L^{\max} when S_t increases, as observed in Table II. Remember, however, that the total number of antennas of the cell-free network $L \cdot N = 512$ is greater than the cellular scenario that has $M = 64$ only.

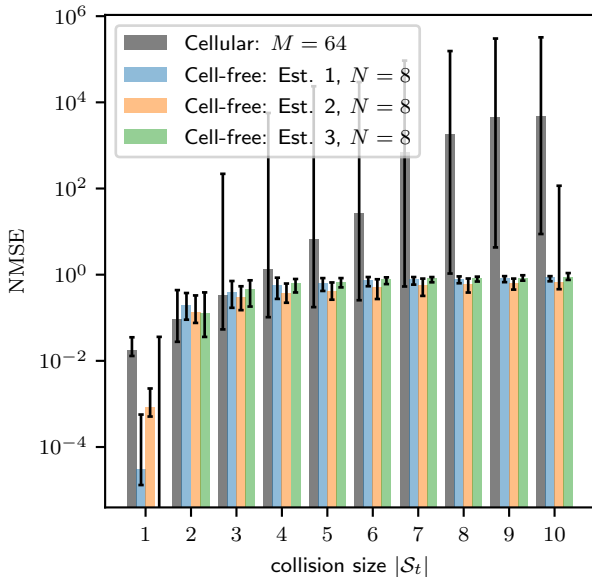


Fig. 5. Comparison of the performance of the estimators for different collision sizes $|S_t|$ in terms of the NMSE metric. The pair of parameters ($|C_k|, L^{\max}$) is selected according to Table II. The colored bars denote the median values, while the error bars correspond to the IQRs.

To evaluate how the performance of the estimators is

dependent on the number of antennas N per AP, we plot Fig. 6 when considering $|S_t| = 2$ colliding UEs. The number of antennas N per AP is crucial to obtain the channel hardening and favorable propagation effects, which are related to the approximations of: **i)** $\frac{1}{N} \|\mathbf{y}_{It}\|_2^2$ in (6) and (25); **ii)** \tilde{z}_k in (14) and (28). There are three main observations we can learn from the figure. First, the cell-free estimators perform really poorly when $L \cdot N = M = 64$ antennas. This means that the total number of antennas $L \cdot N$ on the cell-free network needs to be at least $4\times$ or higher than the number of antennas M at a BS of an "equivalent" cellular mMIMO network. This observation is in line with the discussion carried out in [3], where the authors observed the lower ability to obtain channel hardening and favorable propagation effects in cell-free networks due to magnitude dissimilarities in average channel gains β_{kl} 's. Second, the cell-free estimators tend to underestimate the true α_t in (16) and their estimates are not asymptotically unbiased; where the closer to zero the NEB is, the more unbiased is the estimate. This can be explained by the fact that the estimators rely on the approximation $\sum_{l \in \mathcal{P}_t} \beta_{kl} \approx \sum_{l \in C_k} \beta_{kl}$. This approximation is error passive, as the sum over \mathcal{P}_t is

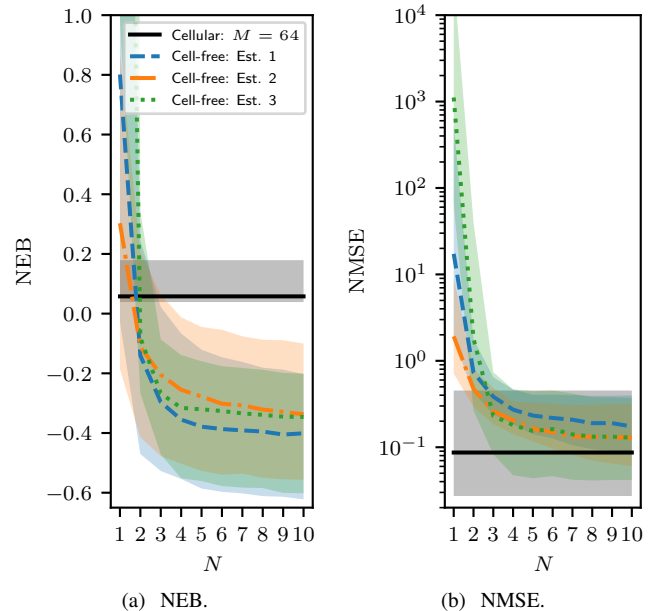


Fig. 6. Evaluation of the performance of the estimators when varying the number of antennas per AP N for a fixed collision size of $|S_t| = 2$ UEs. The pair of parameters ($|C_k|, L^{\max}$) is selected according to Table II for $N = 8$ antennas per AP. The lines stand for the median values, while the colored regions indicate the IQRs.

expected to be a little larger than the sum over C_k as the collision size $|S_t|$ increases, as seen in Fig. 4; and the opposite can be true for small $|S_t|$. Third, the cell-free estimators tend

to achieve an NMSE performance floor after a certain increase in the number of antennas N per AP. Again, this is related to the approximation $\sum_{l \in \mathcal{P}_t} \beta_{kl} \approx \sum_{l' \in C_k} \beta_{kl'}$, and shows that after a certain moment it becomes useless to increase N to improve the performance of the estimators.

Remark 3. (Consequence of Underestimation) *Due to the fact that the UEs tend to underestimate the total UL signal power from colliding UEs α_t in (16), more UEs are expected to declare themselves winners of the contention in (17) of Step 3. Fortunately, the concept of spatial separability introduced in Step 4 can aid the cell-free network to support more UEs.*

E. Selecting Parameters in Practice

From the evaluation of the estimators, we could see the importance of selecting the pair of parameters $(|C_k|, L^{\max})$ to improve their performance. In this part, we will discuss how to select these parameters in such a way as to make it practical to implement the estimators.

1) *Selecting ι or $|C_k|$:* The selection of ι or $|C_k|$ occurs on the UE's side and it affects the quality of the approximation $\sum_{l \in \mathcal{P}_t} \beta_{kl} \approx \sum_{l' \in C_k} \beta_{kl'}$ made to turn the three estimators presented above feasible in practice. We propose two methods to implement such selection: **a) Fixed:** UEs $k \in \mathcal{K}$ realize Step 0 and maintain their knowledge on \check{C}_k unchanged; \check{C}_k is used to obtain the estimates; **b) Greedy Flexible:** UE $k \in \mathcal{K}$ obtains \check{C}_k in Step 0. Then, it evaluates its estimate of $\hat{\alpha}_{t,k}$ by sweeping over all possible sizes of C_k from the maximum $|\check{C}_k|$ to the minimum 1, where $1 \leq |C_k| \leq |\check{C}_k|$. At each size reduction of C_k , the average channel gain $\beta_{kl'}$ for $l' \in C_k$ of smaller magnitude is removed. After this sweep, the k -th UE will have a set of estimates $\{\hat{\alpha}_{t,k}^{(|\check{C}_k|)}, \dots, \hat{\alpha}_{t,k}^{(1)}\}$. With this, UE k evaluates the decision in (17) for each of the obtained estimates. If one of the decisions indicates that the UE must retransmit, UE k decides by R_k ; otherwise, the UE chooses I_k . The idea is to greedily increase the quantity of re-transmissions in order to try to solve them using the concept spatial separability defined in Step 4. *Computational complexity observation:* for both methods, note that $\sum_{l' \in C_k} \beta_{kl'}$ can be computed only once and stored at UE k . This is a valid assumption when APs are stationary and UEs do not change position much. These computations can be realized even when a UE is inactive, avoiding introduction of delay in the RA.

2) *Selecting L^{\max} :* The choice of L^{\max} occurs on the network's side, more specifically at the CPU. This parameter aims to select the most relevant APs to attend each pilot collision \mathcal{S}_t , $\forall t \in \mathcal{T}$. Such selection affects the quality of the approximation \tilde{z}_k in (14) and (28) and, as a consequence, the quality of the estimate $\hat{\alpha}_{t,k}$ obtained at the UEs $k \in \mathcal{K}$. For the selection of L^{\max} , we propose a *training phase* that assumes that the network has a reliable estimate of the number of inactive UEs $|\mathcal{U}|$ and the average collision size $\mathbb{E}\{|\mathcal{S}_t|\}$ given a probability of activation P_a . The procedure to obtain a suitable value for L^{\max} is described in Algorithm 2 and is independent of the estimator choice. In parallel, the training phase can also be used to obtain the compensation factor δ by computing the average of \tilde{q}_l^{avg} and broadcasting this value to the UEs. The training phase needs only to be performed a few

times when, for example, the RA performance drops below a selected threshold indicating a drastic change in network composition.

Algorithm 2 Training phase for selection of L^{\max} .

```

1: Input: Set of inactive UEs:  $\mathcal{U}$ ; Probability of activation:  $P_a$ ; Number of APs:  $L$ ; Number of antennas per AP:  $N$ ; Number of RA pilots:  $\tau_p$ ; Number of random transmission rounds:  $R$ ; Number of transmission repetitions:  $E$  [symbols].
2: Output: Max. number of APs attending each pilot  $L^{\max}$ 
3: Procedure:
4:  $T = R \cdot E$  ▷ calculate training duration in symbols
5: for  $r \leftarrow 1$  to  $R$  do
6:   generate  $\mathcal{K} \subset \mathcal{U}$  given  $P_a$ 
7:   UE  $k \in \mathcal{K}$  selects a pilot  $t \in \{1, 2, \dots, \tau_p\}$  at random
8:   for  $e \leftarrow 1$  to  $E$  do
9:      $|\mathcal{K}|$  UEs transmit their pilots as in eq. (4)
10:    CPU calculates and store  $\tilde{\mathbf{A}} \in \mathbb{R}_+^{\tau_p \times L}$  as per (8)
11:   end for
12:   average out realizations of  $\tilde{\mathbf{A}}$  w.r.t.  $E$ , yielding  $\tilde{\mathbf{A}}$ 
13:    $\tilde{\mathbf{b}}_t \in \mathbb{R}_+^L = [\tilde{\mathbf{A}}]_t$ ; ▷  $t$ -th row of  $\tilde{\mathbf{A}}$ 
14:   for  $t \leftarrow 1$  to  $\tau_p$  do
15:     if  $t$  was used by a UE in  $\mathcal{K}$  as per eq. (6) then
16:        $\epsilon \leftarrow \frac{1}{L} \sum_{l \in \mathcal{L}} \tilde{b}_{tl}$  ▷ average threshold
17:        $L_t \leftarrow \text{sum}(\tilde{\mathbf{b}}_t \geq \epsilon)$  ▷ element-wise comparison
18:        $\tilde{\tau}_p \leftarrow \tilde{\tau}_p + 1$  ▷ aux. variable initialized as 0
19:     end if
20:   end for
21:    $L_r^{\max} \leftarrow \frac{1}{\tilde{\tau}_p} \sum_{t=1}^{\tilde{\tau}_p} L_t$ 
22: end for
23: return  $L^{\max} \leftarrow \lceil \frac{1}{R} \sum_{r=1}^R L_r^{\max} \rceil$ 

```

V. NUMERICAL RESULTS

In this section, we show the effectiveness of the CF-SUCRe protocol by evaluating its performance and energy efficiency (EE). The simulation parameters are the same as the ones reported in Table I, unless stated otherwise. We consider a square coverage area of 400 m \times 400 m and also fix the cell-free architecture to have $L = 64$ APs and the same 8 \times 8 square grid disposition shown in Fig. 2.

A. Baseline Schemes

We adopt two baseline schemes: **a) Ce-SUCRe [3]:** we naturally consider the Ce-SUCRe by [3] as a baseline, which uses the estimator described in Remark 1. For fairness reasons, we fix the DL transmit power of the cell-centered BS to $q = 200$ mW; **b) BCF:** from the concept of spatial separability presented in Step 4, we suggest the following grant-free protocol: 1) UEs in \mathcal{K} transmit their randomly chosen pilots; 2) UEs are only admitted by the network if they are spatially separable according to Algorithm 1. This baseline scheme ignores the SUCRe introduced by Steps 2 and 3. The best performance of BCF is obtained when $L^{\max} = 64$ APs, since this condition increases the probability of a UE being spatially separable. This means that all L APs operate attending all τ_p

pilots for the BCF scheme, that is, user-centric perspective is not entirely exploited.

B. Evaluation Metrics

1) *Performance*: The *average number of access attempts* (ANAA) measures how many accesses on average a UE needs to try so as to successfully be admitted by the network after the first time the UE starts to be in $\mathcal{K} \subset \mathcal{U}$. We set the maximum NAA a UE can realize to 10 attempts and the probability of reattempt in the next coherence block if the attempt fails to 50%. Hence, a UE gives up accessing the network after reaching 10 NAA. While in the Ce-SUCRe from [3], two or more UEs only need to retransmit in Step 3 for the access attempt to fail, Algorithm 1 is used to determine what is considered a failed attempt for the BCF and CF-SUCRe protocols.

2) *EE*: We evaluate the EE on each side: **a) UE's side**: we vary the UL transmit power p and show how the ANAA varies for each of the RA protocols considered; **b) network's side**: we define the *total consumed power* (TCP) for the type of network and the RA protocol in question. For the CF-SUCRe, the TCP is

$$\text{TCP}^{\text{cf}} = \text{ANAA}^{\text{cf}} \cdot \underbrace{(\tau_p + 1)}_{\text{\# of DL symbols}} \cdot \underbrace{(q_l \cdot \bar{\tau}_{pl})}_{\text{total power per AP}} \cdot \bar{L},$$

where the superscript "cf" indicates dependency with the CF-SUCRe protocol, $0 \leq \bar{\tau}_{pl} \leq \tau_p$ is the average number of *active* pilots per AP, and \bar{L} is the average number of *operative* APs. The number of DL symbols corresponds to the sum of: i) τ_p symbols used to respond back to the UEs in Step 2 and ii) 1 symbol used to communicate back with the winning UEs in Step 4. The variables of the metric above change as follows for the considered benchmarks: a) for the CF-SUCRe with Estimator 3, the total power related to the DL response in Step 2 depends on \tilde{q}_l^{avg} instead of q_l ; b) for the Ce-SUCRe protocol, q_l is replaced by q , $\bar{\tau}_{pl}$ is independent of l , and $\bar{L} = 1$; and, c) for the BCF protocol, the number of DL symbols is 1, $\bar{\tau}_{pl}$ is also independent of l , and $\bar{L} = L$ APs.

C. Evaluating Performance

In Fig. 7, we compare the performance of the RA schemes considered in this work. In the figure, we evaluate the two methods proposed to select $|C_k|$ in Subsection IV-E for the CF-SUCRe protocol. Moreover, we consider two performance bounds for the CF-SUCRe: a lower and a practical bound. The *lower bound* considers that the network is able to distinguish collision sizes $|S_t|$ given a realization of the t -th row $[\hat{\mathbf{A}}]_{t,:}$. Given the knowledge of $|S_t|$, the network selects the most appropriate L^{max} based on the "best" median NMSE analysis made in Sub-subsection IV-D3 (*c.f.* Table II). The lower bound establishes the best performance that one can obtain with the CF-SUCRe for each estimator. Further, it motivates the possibility to obtain a more intricate method to select L^{max} than the simple one presented in Algorithm 2. For example, further study of the properties of $\hat{\mathbf{A}}$ can be combined with a machine learning method. The *practical bound* assumes that L^{max} is selected using Algorithm 2.

From Fig. 7, the "greedy flexible" method for selection of the number of APs $|C_k|$ known by a UE k works better than the fixed one in all cases presented. This suggests that increasing the number of collisions and allowing them to be naturally resolved via spatial separability is a good practice. In fact, this is proven by observing that the BCF benchmark outperforms the CF-SUCRe protocol. However, despite the better performance of the BCF, the latter assumes that all L APs are operating in the RA step, while the CF-SUCRe does not. This can dramatically impact the EE, as shall be evidenced in Subsection V-D. From here, we can get an important insight into how the CF-SUCRe works: the protocol adds a control procedure in Steps 2 and 3 that acts as a filter that aims to increase the amount of collisions that can be resolved via spatial separability in Step 4. The idea is that part of the collisions that would not be resolved with spatial separability are resolved or facilitated through the SUCRe rule defined in (17) from Step 3. Such additional control actions also add the possibility to reduce the number of APs $|\mathcal{P}|$ that needs to be operating without affecting collision resolution performance so much. However, this orchestration can also lead to a very low re-transmission rate due to errors introduced by Steps 2 and 3, eventually reducing effectiveness of the spatial-separability-based collision resolution. In other words, the CF-SUCRe protocol combines two collision resolution strategies: the SUCRe rule in (17) and the spatial separability concept in Algorithm 1. The former helps in increasing the capacity to exploit the later and allows the control of the number of operative APs while alleviating performance losses.

Fig. 7 also shows that the cell-free schemes proposed here remarkably outperforms the Ce-SUCRe protocol. Further, for the CF-SUCRe, the difference between the lower and practical bounds is modest. This implies that, despite being simple, the method proposed in Algorithm 2 is effective. However, it still depends on an earlier training stage to be carried out. One can also note that Estimator 3 has the best performance among all estimators for both lower and practical bounds. This is because Estimator 3 tremendously outperforms the other two estimators in the case where there is no collision $|S_t| = 1$ and matches well with the performance of the others as the size of the collisions increases, as shown in Fig. 5.

For a very high number of inactive UEs $|\mathcal{U}| \in [10,000; 35,000]$, we notice that the performance of cell-free methods abruptly deteriorates and becomes comparable to that of the Ce-SUCRe. This abrupt inflection point occurs because: **i)** from a moment on, the concept of spatial separability can no longer be explored, given the fixed number of APs L , the coverage geometry (*e.g.*, density of APs), and specific channel conditions such as path loss, and **ii)** the performance of the estimators becomes unreliable. These two causes indicate why the inflection point is different for the BCF and CF-SUCRe methods. Theoretically, we can better characterize the limitation of spatial separability by finding an estimate for the maximum number of UEs that can be supported by this concept. For the considered scenario, we have that the density of APs is $\rho = L/(400)^2 = 1/2500$ AP per m^2 . Since $d^{\text{lim}} \approx 73.30$ m, it is expected that on average $\rho \cdot \pi \cdot (d^{\text{lim}})^2 \approx 6.75$ APs are serving each UE.

Therefore, considering that all the τ_p pilots are deployed by all L APs and UEs do not share APs, the theoretical maximum number of UEs that can be solved via spatial separability is $\tau_p / (6.75 \cdot P_a) \approx 74,000$ UEs. However, due to the fact that APs are shared by different UEs and the increasing difficulty of separating UEs when the collision size $|\mathcal{S}_t|$ grows, one can conclude that this theoretical value is halved to approximately 34,000 UEs for the BCF scheme. For the CF-SUCRe protocol, this value reduces even more to about 10,000 UEs, since, in addition to spatial separability, the performance of Steps 2 and 3 also suffers from increasing collision sizes $|\mathcal{S}_t|$.

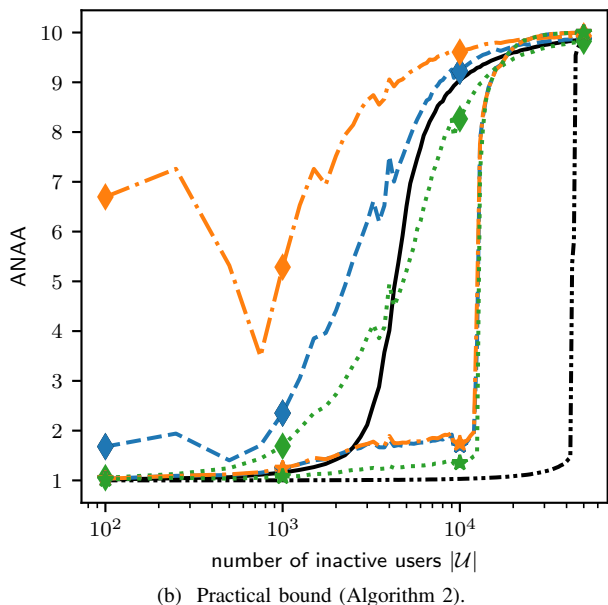
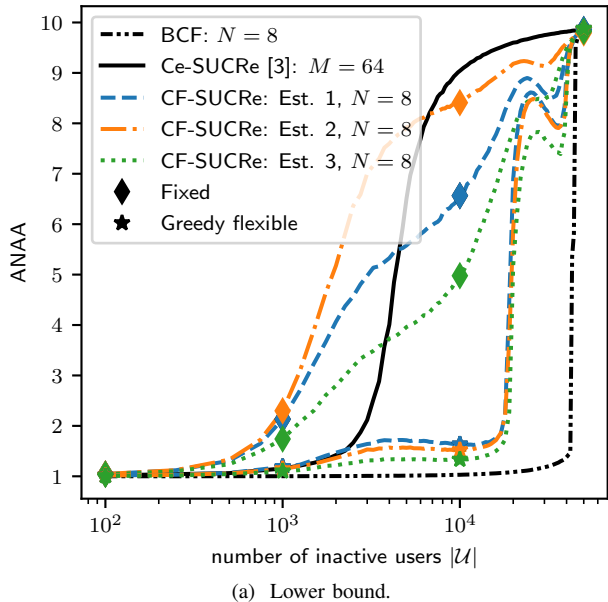


Fig. 7. Performance evaluation of RA methods: BCF, Ce-SUCRe [3], and CF-SUCRe. The two selection methods of $|\mathcal{C}_k|$ are assessed for CF-SUCRe: fixed and greedy flexible. The cell-free mMIMO network is comprised of $L = 64$ APs disposed in a 8×8 square grid layout. Important fixed parameters are: $\tau_p = 5$ pilots, $P_a = 0.1\%$, maximum number of attempts is 10, and probability of reattempts is 50%. Other parameters are available in Table I.

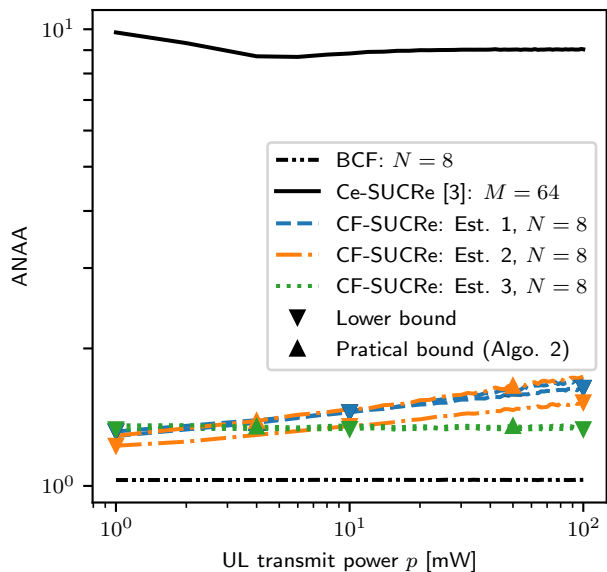
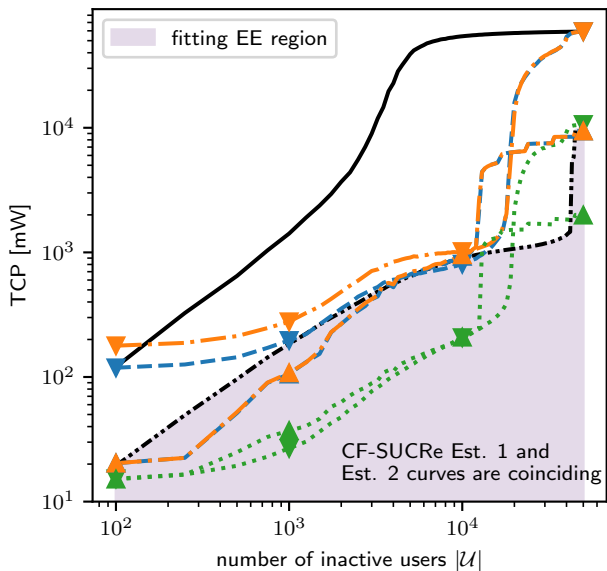
D. Evaluating Energy Efficiency

Fig. 8 evaluates the EE of the RA schemes discussed here considering both the UE's and the network's sides. For the UE's side, while the performance of Ce-SUCRe worsens for the case of $p = 1$ mW compared to $p = 100$ mW, the performance of cell-free schemes changes little or even improves when decreasing the UL transmit power p . Due to the fact that APs tend to be closer to UEs, cell-free protocols allow the use of lower UL transmit powers, savings UEs' battery life. Using lower p 's can also decrease interference in CF-SUCRe estimates, supporting the observed gains. However, how much the UL transmit power p can be reduced needs to be better characterized, since this value cannot be so small as to make the decoding of the UEs' signal by the APs unfeasible. Finally, p can be further optimized to improve protocol performance given the decoding constraints.

For the network's side evaluated in Fig. 8b, we note even more intriguing results for the TCP metric. Clearly, our proposed cell-free protocols are more energy efficient than the Ce-SUCRe, mainly because their performance is really superior. But also because, in the case of CF-SUCRe, not all APs need to be operating. This gain becomes even clearer when comparing the TCP curves of the BCF and CF-SUCRe schemes. The BCF protocol uses all $L = 64$ APs to attend the pilots. In contrast, the CF-SUCRe does not, which explains why the total consumed power related to the CF-SUCRe schemes can be even lower than that of the BCF scheme operating under certain scenarios, even with the BCF performing better in Fig. 7. Therefore, despite the higher overhead, the proposed CF-SUCRe schemes (Est. 1, 2, and 3) can be more energy efficient than the BCF, as the average number of operative APs participating in RA is reduced while maintaining reasonable performance. The hatched region in Fig. 8b illustrates the EE region of interest in which CF-SUCRe may be a more interesting method than BCF from the energy efficiency point-of-view. Interestingly, Estimator 3 exhibits the best EE gains, due to the reduced effective DL transmit power \tilde{q}_{lt} in (27). This fact together with the best performance attained by the Est. 3 in Fig. 7a motivate the use of the CF-SUCRe scheme with Est. 3 in a wide range of practical scenarios of interest.

VI. CONCLUSIONS

In this work, we considered the extension of the SUCRe to cell-free mMIMO networks aiming to explore the user-centric perspective. As we carry out such an extension, we observed that the macro-diversity introduced by the cell-free network can naturally help in the resolution of collisions. With that, we introduced the concept of spatial separability. Then, we proposed two RA protocols: i) the grant-free BCF that only resolves collisions via spatial separability and ii) the grant-based CF-SUCRe that combines SUCRe and spatial separability collision resolutions. For the CF-SUCRe to be implementable, we introduced three estimators to perform SUCRe, two methods to control the preferred subset of APs known by the UEs (fixed and greedy flexible), and one method to control the preferred subset of APs that serves each pilot

(a) UE's side for $|\mathcal{U}| = 10,000$ inactive UEs.

(b) Network's side.

Fig. 8. EE evaluation of RA methods: BCF, Ce-SUCRe [3], and CF-SUCRe. Only the *greedy flexible method* of $|\mathcal{C}_k|$ is assessed. The cell-free mMIMO network is comprised of $L = 64$ APs disposed in a 8×8 square grid layout. Fixed parameters: $\tau_p = 5$ pilots, $P_a = 0.1\%$, max. # of attempts is 10, and probability of reattempts is 50%. Other parameters are available in Table I.

(Algorithm 2). Our numerical results revealed that our cell-free RA protocols exceedingly outperforms the Ce-SUCRe from [3] under an "equivalent" cellular mMIMO network. For example, the average EE of CF-SUCRe compared to that of the Ce-SUCRe is $125\times$ lower, reaching of up to $300\times$ in some settings. Moreover, despite the additional overhead, CF-SUCRe adopting Estimator 3, greedy flexible, and Algorithm 2 performs as well as the BCF under an extensive region determined by the number of inactive UEs $|\mathcal{U}|$; but with an average EE $3\times$ smaller.

APPENDIX PROOF OF THEOREM 1

We solve (22) with the method of Lagrange multipliers. The Lagrange function is:

$$\mathcal{L}(\alpha_t, \mu) = f(\alpha_t) - \mu g(\alpha_t), \quad (33)$$

where μ is a constant known as the Lagrange multiplier. To introduce the constraint into the solution, we have to check the constraint feasibility with the following equality: $\nabla_{\alpha_t} f(\alpha_t) = \mu \nabla_{\alpha_t} g(\alpha_t)$. The gradients are:

$$\nabla_{\alpha_t} f(\alpha_t) \in \mathbb{R}_+^{|\mathcal{P}_t|} = \mathbf{1}, \quad (34)$$

$$[\nabla_{\alpha_t} g(\alpha_t)]_l \in \mathbb{R}_+ = \frac{1}{2} \frac{\sqrt{q_l p_k} \tau_p \beta_{kl}}{(\alpha_{lt} + \sigma^2)^{3/2}}, \quad \forall l \in \mathcal{P}_t. \quad (35)$$

Solving $\nabla_{\alpha_t} f(\alpha_t) = \mu \nabla_{\alpha_t} g(\alpha_t)$ for α_{lt} , we get:

$$\alpha_{lt} = \left(\frac{\mu}{2} \sqrt{q_l p_k} \tau_p \beta_{kl} \right)^{2/3} - \sigma^2. \quad (36)$$

Substituting the above equation into the constraint $g(\alpha_t)$ gives

$$\left(\frac{\mu}{2} \right)^{2/3} = N \left(\frac{\sum_{l \in \mathcal{P}_t} (\sqrt{q_l p_k} \tau_p \beta_{kl})^{2/3}}{\mathfrak{R}(z_k)} \right)^2. \quad (37)$$

Plugging the value of $(\mu/2)^{2/3}$ into α_{lt} completes the proof.

REFERENCES

- [1] P. Popovski, *Wireless Connectivity: An Intuitive and Fundamental Guide*. Wiley, may 2020. [Online]. Available: <https://onlinelibrary.wiley.com/doi/book/10.1002/9781119114963>
- [2] A.-S. Bana, E. de Carvalho, B. Soret, T. Abrão, J. C. Marinello, E. G. Larsson, and P. Popovski, "Massive MIMO for internet of things (IoT) connectivity," *Physical Communication*, vol. 37, p. 100859, 2019. [Online]. Available: <https://www.sciencedirect.com/science/article/pii/S1874490719303891>
- [3] E. Björnson, E. de Carvalho, J. H. Sørensen, E. G. Larsson, and P. Popovski, "A random access protocol for pilot allocation in crowded massive MIMO systems," *IEEE Transactions on Wireless Communications*, vol. 16, no. 4, pp. 2220–2234, 2017.
- [4] J. C. Marinello, T. Abrão, R. D. Souza, E. de Carvalho, and P. Popovski, "Achieving fair random access performance in massive MIMO crowded machine-type networks," *IEEE Wireless Communications Letters*, vol. 9, no. 4, pp. 503–507, 2020.
- [5] E. D. Carvalho, A. Ali, A. Amiri, M. Angelichinoski, and R. W. Heath, "Non-stationarities in extra-large-scale massive MIMO," *IEEE Wireless Communications*, vol. 27, no. 4, pp. 74–80, 2020.
- [6] O. S. Nishimura, J. C. Marinello, and T. Abrão, "A grant-based random access protocol in extra-large massive MIMO system," *IEEE Communications Letters*, vol. 24, no. 11, pp. 2478–2482, 2020.
- [7] Ö. T. Demir, E. Björnson, and L. Sanguinetti, *Foundations of user-centric cell-free massive MIMO*. Now Publishers, 2021, vol. 14, no. 3-4.
- [8] U. K. Ganesan, E. Björnson, and E. G. Larsson, "An algorithm for grant-free random access in cell-free massive MIMO," in *2020 IEEE 21st International Workshop on Signal Processing Advances in Wireless Communications (SPAWC)*, 2020, pp. 1–5.
- [9] M. Henriksson, O. Gustafsson, U. K. Ganesan, and E. G. Larsson, "An architecture for grant-free random access massive machine type communication using coordinate descent," in *2020 54th Asilomar Conference on Signals, Systems, and Computers*, 2020, pp. 1112–1116.
- [10] Z. Chen, F. Söhrabi, and W. Yu, "Sparse activity detection in multi-cell massive MIMO exploiting channel large-scale fading," *IEEE Transactions on Signal Processing*, vol. 69, pp. 3768–3781, 2021.
- [11] U. K. Ganesan, E. Björnson, and E. G. Larsson, "Clustering based activity detection algorithms for grant-free random access in cell-free massive MIMO," *IEEE Transactions on Communications*, pp. 1–1, 2021.